© 2014. Published by The Company of Biologists Ltd | The Journal of Experimental Biology (2014) 217, 1563-1569 doi:10.1242/jeb.097816

RESEARCH ARTICLE

Temperature mediates the effect of humidity on the viscoelasticity of glycoprotein glue within the droplets of an orb-weaving spider's prey capture threads

Sarah D. Stellwagen*, Brent D. Opell and Kelly G. Short

ABSTRACT

Sticky viscous prey capture threads retain insects that strike araneoid orb-webs. The threads' two axial fibers support a series of glue droplets, each featuring a core of adhesive viscoelastic glycoprotein covered by an aqueous solution. After sticking, the glue extends, summing the adhesion of multiple droplets, and dissipates some of the energy of a struggling prey. As a day progresses, threads experience a drop in humidity and an increase in temperature, environmental variables that have the potential to alter thread and web function. We hypothesize that thread droplets respond to these opposing environmental changes in a manner that stabilizes their performance, and test this by examining threads spun by *Argiope aurantia*, a species that occupies exposed, weedy habitats. We confirmed that decreased humidity increases glycoprotein viscosity and found that increased temperature had the opposite effect. To evaluate the combined effect of temperature and humidity on a droplet's ability to transfer adhesive force and dissipate energy, we extended a droplet and measured both the deflection of the axial line supporting the droplet and the duration of its tensive load. The cumulative product of these two indices, which reflects the energy required to extend a droplet, was greatest under afternoon (hot and dry) conditions, less under morning (cool and humid) conditions, and least under hot and humid afternoon conditions. Although the opposing effects of temperature and humidity tend to stabilize glycoprotein performance, *A. aurantia* thread droplets appear to function optimally during the afternoon, equipping this species to capture large orthopterans, which are most active at this time.

KEY WORDS: *Argiope aurantia*, Biomaterial, Glycoprotein, Hygroscopic, Viscoelastic

INTRODUCTION

All animals produce glycoproteins, but few incorporate them as adhesive in traps that capture prey. Onychophorans squirt a sticky substance supported by proteinaceous threads onto nearby prey; however, this material is not extruded prior to prey encounter (Betz and Kölsch, 2004). Marine gastropods in the genus *Dendropoma* deploy sticky mucus nets that gather suspended plankton and detritus (Kappner et al., 2000). Modern orb-weaving spiders incorporate viscoelastic glycoprotein glue in the spiral capture threads of their webs (Fig. 1). This system is unique in several ways; the adhesive is a crucial part of an aerial filtering system and its production anticipates future prey. Unlike onychophoran adhesive, which is produced when needed, or gastropod mucus, which remains in an osmotically and thermally stable marine environment, spider thread glycoproteins must function over the course of a day where ambient temperature and humidity oscillate, often dramatically (Fig. 2).

Three spinning spigots on each of an orb-weaving spider's paired posterior lateral spinnerets produce its composite viscous capture threads. A single flagelliform spigot produces a supporting protein axial line (Sekiguchi, 1952), which is coated by material from two adjacent aggregate glands as it emerges (Apstein, 1889). The two coated lines from each spigot merge to produce a cylindrical, proto viscous thread (Warburton, 1890). Low molecular weight molecules and inorganic salts in the fluid surrounding the axial lines rapidly attracts atmospheric moisture, increasing the cylinder's volume and surface tension, setting the stage for Plateau–Rayleigh instability to form the cylinder into droplets (Plateau, 1873; Boys, 1889; Rayleigh, 1892; Edmonds and Vollrath, 1992). Within each droplet, an adhesive glycoprotein core forms and remains covered by a hygroscopic aqueous outer layer that also covers axial lines in the thread's inter-droplet region (Opell and Hendricks, 2009) (Fig. 1C).

Thread adhesion is enhanced by the extensibility of both the glycoprotein cores within droplets (Sahni et al., 2010) and the axial lines (Opell et al., 2008). As force is applied to a thread that has contacted a surface, these droplets extend, permitting the axial line to sum their adhesive forces (Opell and Hendricks, 2007; Opell and Hendricks, 2009). The contribution of glycoprotein to this suspension bridge mechanism depends on a combination of viscosity that absorbs energy through hysteresis (Gosline et al., 1986) or dissipates energy upon droplet pull off (Sahni et al., 2010) and the reversible elastic deformations that retain prey in the web after interception (Sahni et al., 2010). These qualities, which contribute to the overall prey capture success of the web, have the potential to be altered by ambient conditions.

The hygroscopic aqueous material that coats the glycoprotein and axial lines of viscous threads absorbs atmospheric moisture and transfers this moisture to the glycoprotein glue (Opell et al., 2011b). Water absorbed by this outer layer during periods of high humidity [greater than ~60% relative humidity (RH)] causes over-lubrication (over-hydration) of the glue in *Argiope aurantia* Lucas 1833, reducing adhesion (the energy required to pull a droplet from a surface) through the disruption of hydrogen bonding and electrostatic interactions of the glycoprotein molecules, as Sahni and colleagues (Sahni et al., 2011) also show for *Larinioides cornutus*. However, threads of the nocturnal *Neoscona crucifera*, found in humid habitats, do not exhibit an upper humidity threshold (Opell et al., 2013). This suggests that the glycoprotein is an adaptable material, whose properties are selected to suit a species' habitat.

Argiope aurantia is an active daytime predator that prefers open, grassy habitats and, in our area of southwestern Virginia, USA,

Department of Biological Sciences, Virginia Tech, Blacksburg, VA 24061, USA.

*Author for correspondence (sstellw@vt.edu)

Received 1 October 2013; Accepted 13 January 2014

The Journal of Experimental Biology (2014) doi:10.1242/jeb.097816

List of abbreviations

DE	droplet extension
PE	pre-extension
TLT	total loaded time

matures in late summer. Their webs are available to capture prey in the early morning as soon as enough webbing is produced for interception. Webs of adult females are usually recycled daily; however, individuals may occasionally wait several days before replacing a web (Reed et al., 1969). Females continuously occupy the center of the web and only leave to capture prey, seek shelter during hazardous weather, and to deposit egg sacs. During the early morning, webs experience low, late summer and early autumn temperatures (15–20°C) and high relative humidities (90–100% RH). As the day progresses, temperatures rise as high as 35–40°C, while RH often drops to 45% or below (Fig. 2). This normal cycling of temperature and humidity is sometimes interrupted by periods of rainy weather, resulting in unusually high daytime humidity (Fig. 2, 5–7 August). Although *A. aurantia* forage from morning to evening, the bulk of their prey is captured during the afternoon, when large orthopterans are the most active and likely to be captured (Harwood, 1974).

As *A. aurantia* webs function over the course of a day when temperature and humidity vary greatly, the goal of this study is to examine the combined effect of these environmental factors on the properties of their glycoprotein adhesive. When temperature drops, viscous materials become stiffer, requiring either more force or more time to undergo deformation. Therefore, low temperatures may increase the viscosity of a spider web's adhesive droplets, resulting in stiffer glue and increased energy absorption during glycoprotein extension. However, the temperature increase that causes glycoprotein to become more pliable is usually accompanied by a decrease in humidity, which reduces glycoprotein hydration, extensibility and the potential for over-lubrication. Therefore, we hypothesize that temperature and humidity act in an antagonistic fashion, which tends to stabilize glycoprotein function over the course of a day. We test this by measuring the performance of viscous droplets from the webs of *A. aurantia* under conditions that simulate cool and humid mornings, hot and dry afternoons, and hot and humid afternoons.

RESULTS

In contrast to previous studies that measured total droplet extension (Opell et al., 2011b; Opell et al., 2013), we focused on the time during which an extending thread droplet was under tension, reasoning that non-loaded glycoprotein filaments that occasionally persist after the filament is no longer under an observable tension contributed neither to thread adhesion nor to energy dissipation. We used angular deflection of a thread's axial line (Fig. 3) to quantify the tension on droplets that remained consolidated before extending (pre-extension phase, Fig. 4) and during extension (droplet extension phase), with a 180 deg angle denoting a non-loaded condition. This angle also provided a means of comparing the impact of temperature and humidity on glycoprotein viscosity, as axial line deflection at the initiation of droplet extension is inversely proportional to glycoprotein viscosity. Plotting this angular index (y-axis) against the time in seconds at which each angle was measured produces a plot (Fig. 4) that is similar to a stress–strain curve, with the area under the line being proportional to the energy required to extend a droplet. These curves provide a convenient way to compare droplet performance under the three experimental conditions.

Table 1 presents mean droplet dimensions (length, width and volume) for droplets in the three treatment groups. The first set of values averages the means of five droplets from each of the 13 individuals and includes the two extended droplets. The second set includes only the averages of each individual's two extended droplets. When log transformed, the droplet length, width and volume for each treatment were normally distributed; however, the trend for these dimensions to increase with humidity was not significant (ANOVA, $P>0.36$).

Table 2 compares the duration of total loaded time (TLT), pre-extension (PE) and droplet extension (DE) phases and the axial line deflection angles at five intervals during DE for the three experimental conditions. The TLT for droplets exposed to afternoon conditions was 29.3 s, which is 28% longer than morning conditions (22.9 s) and 67% longer than combined hot and humid (hereafter 'hot & humid') conditions (17.5 s) (Student's t, $P=0.0233$ and <0.0001, respectively). Thus, a 10°C rise in temperature increased TLT by 5.4 s (24%) whereas a 35% decrease in RH increased TLT by 11.8 s (40%). When an individual's mean droplet volume prior to extension was averaged across the three temperature/humidity treatments, droplet volume was

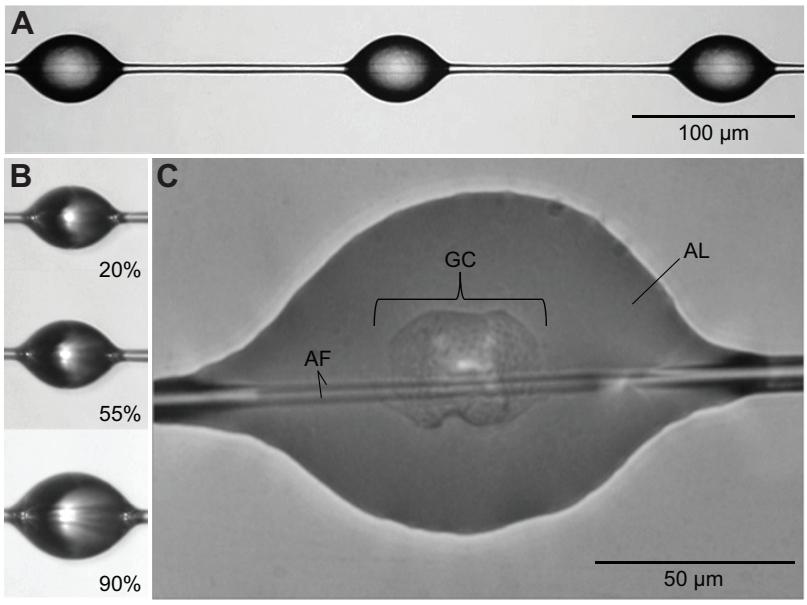

Fig. 1. *Argiope aurantia* viscous silk. (A) Glue droplets suspended on the supporting axial thread; (B) a single droplet exposed to increasing humidity, demonstrating the hygroscopic properties of the aqueous material; and (C) a flattened droplet showing the pair of supporting axial fibers (AF), outer aqueous layer (AL) and the inner glycoprotein core (GC).

The Journal of Experimental Biology (2014) doi:10.1242/jeb.097816

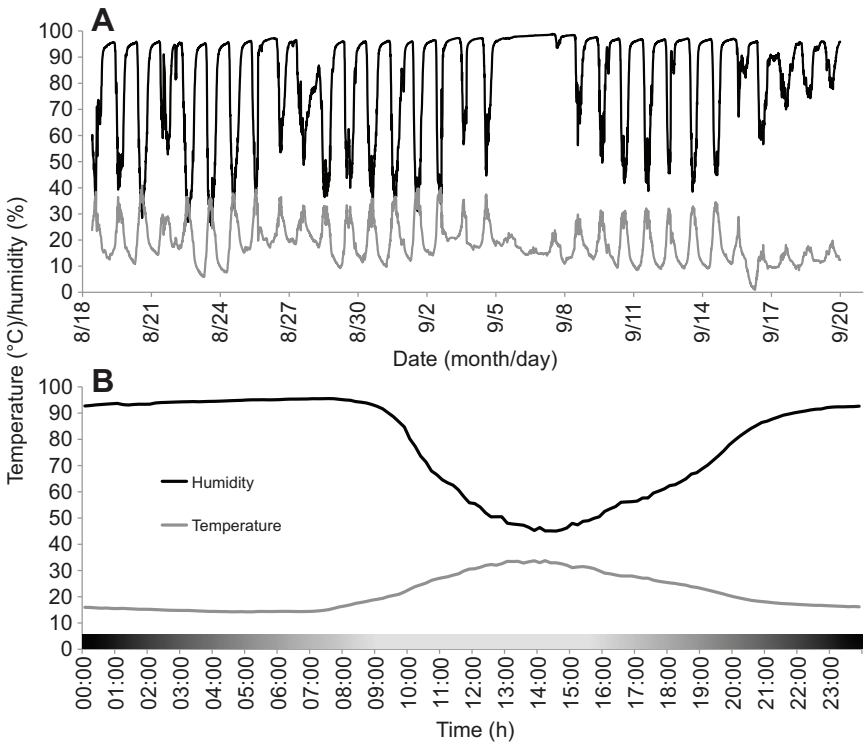

Fig. 2. Humidity and temperature changes at the Heritage Park collecting site for *Argiope aurantia*. These data were collected 18 August–19 September 2011 (A), and averaged over a 24 h period from 18 August to 6 September (B).

directly related to the angle at the initiation of droplet pull off, inversely related to TLT and unrelated to DE (P=0.0320, 0.0317 and 0.5306, respectively). This indicates that as a droplet incorporates more atmospheric moisture, the glycoprotein becomes more dilute, less force is required to initiate filament extension and the filament more quickly attains a non-loaded length.

The pre-extension phase differed between the afternoon and hot & humid conditions, while the morning condition did not differ from either the afternoon or hot & humid conditions (Student's t, P=0.0085, 0.1079 and 0.2631, respectively). Under afternoon conditions, droplet pre-extension comprised 71% of the total loaded time (Fig. 5). This increased to 75% under morning conditions and 85% under hot & humid conditions. During the afternoon condition, the extension phase was longer than during the morning and hot & humid conditions; however, the latter two conditions did not differ (Student's t, P=0.0219, 0.0035 and 0.4729, respectively).

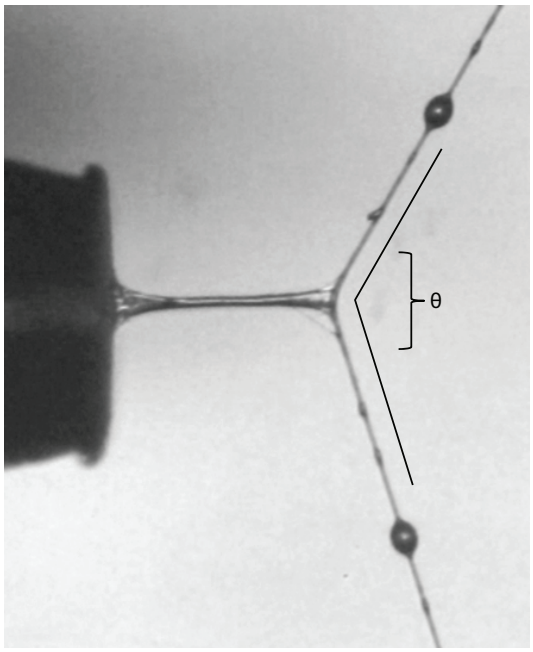

Fig. 3. An extending droplet filament showing the angle of axial line deflection (θ).

Axial line deflection at the initiation of droplet extension (DE time 0) decreased from hot & humid conditions to morning conditions to afternoon conditions (ANOVA, P=0.0328), denoting a progressive increase in the tension on the glycoprotein core required to initiate filament extension as glycoprotein viscosity increased (Table 2, Fig. 6). This was associated with a progressive increase in the duration of the pre-extension phase (ANOVA, P=0.0287), as more time was required to generate the increased tension on axial lines necessary to initiate droplet extension (Table 2). Under all three conditions, axial line deflection decreased during the DE phase (ANOVA or Wilcoxon, P<0.008; Table 2, Fig. 6). As extension progressed, deflections at 25% and 50% under afternoon conditions differed from morning and hot & humid conditions, and at 75% and 99% differed from hot & humid conditions, although morning and hot & humid conditions did not differ (Wilcoxon each pair; Table 2). The total change in angular deflection was remarkably similar among treatments (ANOVA, P=0.9432; Table 2, Fig. 6), exhibiting only an offset in the initiating angle. Under afternoon conditions, the rate of angular change was linear, and under morning and hot & humid conditions most of the change occurred during the first half of loaded droplet extension.

As axial line deflection is proportionate to the tension on an extending droplet filament, the cumulative product of axial line deflection and the duration of loaded droplet extension is proportional to the energy required to extend a droplet. Plots of these values show that 25% more energy is required to extend a droplet under morning than under hot & humid conditions, and 58% more energy is required to extend a droplet under afternoon conditions than under morning conditions (Fig. 6).

The Journal of Experimental Biology (2014) doi:10.1242/jeb.097816

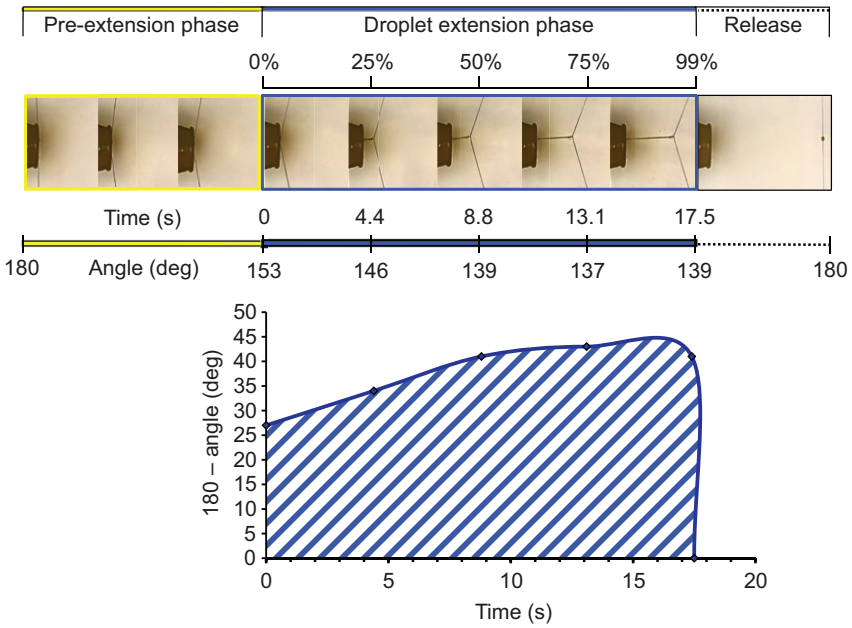

Fig. 4. The phases of droplet loading, as indicated by axial line deflection. The pre-extension phase starts when the supporting axial line is 180 deg and finishes when the droplet begins to extend. The droplet extension phase begins when the droplet starts to extend and ends when the axial line resumes its 180 deg position. Before being plotted, angle values were subtracted from 180 deg to indicate an increase in line tension. The area under the curve represents the energy dissipated during droplet extension.

DISCUSSION

Viscous thread performance has been measured by the force required to pull a thread from a surface (Agnarsson and Blackledge, 2009; Opell and Hendricks, 2009) and by the energy required to do so (Sahni et al., 2010; Sahni et al., 2011). Our results allow us to gauge the affect of environmental conditions on both measures of droplet performance. Pre-extension time is directly related to the force required to initiate droplet extension and axial line deflection at the initiation of droplet extension is inversely related to this force. The area under the axial line deflection/loaded extension time curve represents the energy required to complete loaded droplet extension (Fig. 6). As hypothesized, environmental conditions impact both measures of *A. aurantia* droplet performance. Like increased humidity, increased temperature reduced glycoprotein viscosity and, thereby, decreased the force required to initiate droplet extension, the duration of droplet extension times, the tension on extending droplet filaments and the energy required to extend droplets.

Under hot and dry afternoon conditions, initiation of droplet extension required the greatest force and droplet extension required the most energy (Table 2, Fig. 6). Under cool and humid morning conditions, less force and less energy were required. Although the least force and energy was required under hot & humid afternoon conditions, these values were more similar to those of morning conditions than the latter was to afternoon conditions. Thus, under afternoon conditions, droplet extension has the potential to dissipate the greatest amount of energy from struggling prey (Fig. 6), suggesting that the viscous glue droplets function optimally during this time. Although the ability to dissipate energy is lower under morning conditions (Fig. 6), lower temperatures help to stabilize droplet and thread function and facilitate prey capture during this time.

The effect of humidity, which has been documented previously (Opell et al., 2011b; Sahni et al., 2011; Opell et al., 2013), was greater than that of temperature. A 35% increase in RH produced a 14.2 deg increase in axial line deflection at the initiation of droplet extension, whereas a 10°C increase in temperature produced only a 6.1 deg increase in axial line deflection at the initiation of droplet extension (Table 2). This is also clearly seen in the progression of axial line deflection during the droplet extension phase (Fig. 6), where the difference between afternoon and hot & humid conditions is the result of a 35% RH difference and the difference between morning and hot & humid conditions is the result of a 10°C difference. Thus, decreasing humidity and increasing temperature experienced by webs during the afternoon affect viscous threads in opposite ways, but these changes are not strictly compensatory.

Spiders need time to assess, locate and subdue prey intercepted by their webs. Large orb-weavers such as *A. aurantia* rely extensively on large orthopteran prey captured during the afternoon (Harwood, 1974), and these prey can quickly escape from the web. A study examining the escape rates of insects in webs demonstrated

Table 1. Dimensions of suspended droplets for the three treatment groups

	Afternoon 30°C/50% RH	Morning 20°C/85% RH	Hot & humid 30°C/85% RH	ANOVA *P*-value
Droplet volume (five droplets)				
Droplet length (μm)	57.1 ± 11.2	63.5±14.3	63.6±14.3	0.3641
Droplet width (μm)	38.0±8.1	42.7±10.6	41.5±10.3	0.4627
Droplet volume (μm^3)	40,253±28,787	57,429±43,988	54,836±39,251	0.4524
Droplet volume (two extended droplets)				
Droplet length (μm)	57.9±14.2	62.6±14.0	61.6±13.2	0.6029
Droplet width (μm)	39.3±10.6	42.9±10.3	40.8±8.9	0.6084
Droplet volume (μm^3)	45,546±40,076	57,302±44,682	49,854±34,950	0.5874

RH, relative humidity.
n=13 for each treatment; values were log transformed before analysis. Data are means ± 1 s.d.

The Journal of Experimental Biology (2014) doi:10.1242/jeb.097816

Table 2. Extension phase times and angle measurements for each of the three treatment groups

	Afternoon 30°C/50% RH	Morning 20°C/85% RH	Hot & humid 30°C/85% RH	ANOVA *P*-value
Extension time				
Total load (s)	29.3±6.7	22.9±8.7	17.5±4.4	0.0001
Student's *t*	a	b	b	
Pre-extension (s)	20.8±5.4	17.2±6.9	14.8±4.0	0.0287
Student's *t*	a	a,b	b	
Extension (s)	8.5±4.9	5.7±5.8	2.75±1.5	0.0094
Student's *t* (log transformed)	a	b	b	
Axial line deflection				
Angle at time 0 (deg)	127.2±13.3	135.3±15.9	141.4±9.8	0.0328
Student's *t*	a	a,b	b	
Angle at 25% (deg)[a]	133.9±15.1	151.3±17.6	153.0±9.4	0.0053
Angle at 50% (deg)[a]	143.3±18.7	159.2±16.9	161.3±10.4	0.0328
Wilcoxon each pair	a	b	b	
Angle at 75% (deg)[a]	150.5±20.0	163.1±17.5	168.7±10.2	0.0407
Angle at 99% (deg)[a]	157.5±19.5	167.2±15.0	173.3±8.5	0.0671
Wilcoxon each pair	a	a,b	b	
Angular change ($T_{0\%}$–$T_{99\%}$)	30.3±15.3	31.8±14.8	31.9±9.2	0.9432

$T_{0\%}$ and $T_{99\%}$ are averages of the Time at 0% extension and averages of the Time at 99% extension, respectively.
n=13 for each treatment. Data are means ± 1 s.d.
[a]*P*-values are from the Wilcoxon signed rank test.

that of the large, energetic insects that were intercepted by *A. aurantia* webs, 18% escaped in less than a second (Blackledge and Zevenbergen, 2006). Consequently, the length of time that thread droplets can maintain a load while being extended is crucial. Moreover, it is during this extension phase that energy from a struggling prey is dissipated through hysteresis, which occurs when droplets extend and contract.

The rate of droplet strain that we used (69.6 µm s^{-1}) was in the upper range of values used in other studies [1, 10, 50 and 100 µm s^{-1} (Sahni et al., 2010; Sahni et al., 2011)]. In both of these studies, conducted at a 25°C, increased strain rates increased the stress and strain on extending droplets. In the latter study, the maximum stress and strain achieved for each strain rate increased when humidity increased from 15% to 40%, and then decreased from 40% to 90%; however, the relative response to each strain rate remained consistent. Therefore, we believe that, similar to humidity, temperature acts to shift but not reorder the response of viscous droplets to strain rate; however, the strain rate at which viscous threads have been selected to function has not been evaluated.

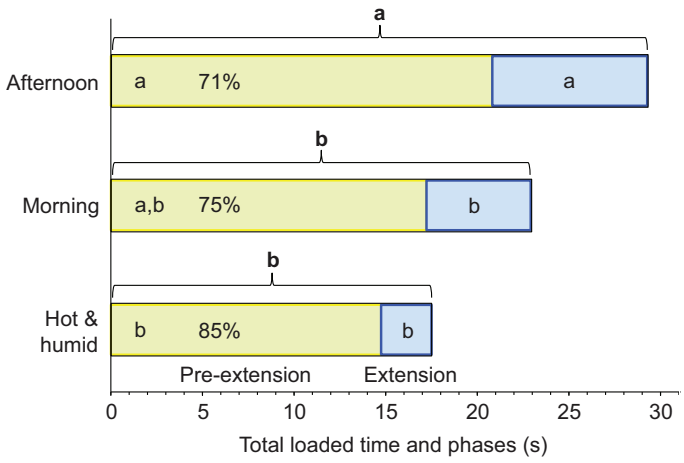

Fig. 5. Total loaded time divided into pre-extension (yellow) and extension (blue) phases for the three treatment conditions. Percentages indicate the total loaded time during the pre-extension phase. Letters designate statistical ranking of total loaded time and individual phases, as documented in Table 2.

The molecular structure of spider glue glycoprotein from *Nephila clavipes* is thought to incorporate components that are similar to those of mucin glycoprotein (Tillinghast et al., 1992; Choresh et al., 2009), which is highly *O*-glycosylated (Rhodes and Ching, 1993). These carbohydrate side chains of glycoproteins are very hydrophilic and usually have all possible hydrogen bonds fulfilled with either water molecules or neighboring saccharides (Cambillau, 1995). One to three water molecules can act as bridges between a saccharide and a protein, establishing a network of viscous material in and around the glycoprotein (Cambillau, 1995). Opell and colleagues (Opell et al., 2013) suggested that over-lubrication in high humidity is due to water molecules providing alternate bonding sites, and disrupting secondary molecular structure of the glycoprotein glue. At optimum humidity, water molecules may keep some carbohydrate moieties 'open' by establishing bonds with them, while still allowing intramolecular structural stability. When a web intercepts an insect, these open carbohydrates may dissociate from the water to form bonds with polar cuticle and cuticular protrusions such as setae (Opell and Schwend, 2007). It may be that at lower temperatures, intramolecular hydrogen bonding within the glycoprotein becomes more stable, decreasing the bonding potential of water molecules with the carbohydrate side chains, and helping to stabilize the glycoprotein glue as its water content increases.

Orb-webs constructed by large spiders such as *A. aurantia* have been selected to withstand the impacts of large, often fast-flying, highly profitable prey (Blackledge and Eliason, 2007; Sensenig et al., 2010; Harmer et al., 2011; Kelly et al., 2011; Sensenig et al., 2013). This is achieved principally through the energy absorbing toughness of the web's non-sticky radial lines, with viscous threads making only a minor contribution (Sensenig et al., 2012). Consequently, these viscous threads have been largely selected for prey retention (Blackledge and Eliason, 2007). The hygroscopicity that is responsible for viscous droplet formation continues to impact the performance of viscous treads over the course of a day and has the potential to adapt a species' web to its environment. A

The Journal of Experimental Biology (2014) doi:10.1242/jeb.097816

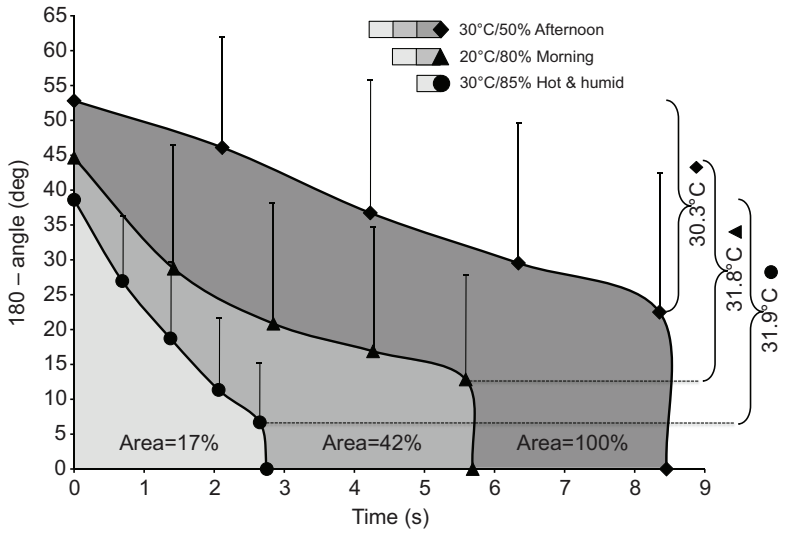

Fig. 6. Axial line deflection at 0, 25, 50, 75, 99 and 100% of loaded droplet extension under each experimental condition. The range of values for each condition is shown at the right. As axial line deflection is proportionate to the tension on an extending droplet filament, the area under each curve represents the energy required to extend a droplet. Standard deviations are represented by the upper bars for the three treatments.

previous study (Opell et al., 2013) showed that the high hygroscopicity of *A. aurantia* threads adapts this species' threads to the low humidity of their exposed habitats. Our study suggests that these threads have also been selected to function optimally at times of the day when they have the greatest chance of intercepting large prey, with low afternoon humidity restoring some of the glycoprotein's viscosity lost to the typically higher temperature at this time of the day.

MATERIALS AND METHODS

Thread collection

We sampled the orb-webs constructed by 13 adult female *A. aurantia* found near Blacksburg, Montgomery County, VA, USA, from 31 August to 18 October 2012. Samples were collected between 05:30 and 09:30 h and analyzed by 16:00 h of the same day. One sector of each spider's web was collected on a 17 cm diameter aluminium ring with a bar across the center. The 5 mm wide ring and bar were covered with Scotch® double-sided tissue tape (Tape 4101T; 3M, St Paul, MN, USA), which adhered to web sectors, maintaining the threads at their native tension. When web sectors were collected, threads extending from the ring were cut with scissors to avoid distorting the sample when the ring was withdrawn from the web. We placed web-sampling rings in a closed plastic container for transport to the laboratory. Each web location was marked with flagging tape to prevent an individual's web from being resampled.

From each spider's web sector we transferred two viscous thread strands to a microscope slide sampler used for each of the three temperature/humidity treatments. We measured the extension of one droplet on each strand and the length (dimension parallel to axial line) and width of these two droplets plus three additional droplets per individual. An individual's extension and droplet volume measurements were averaged to give an operational sample size of 13 for each temperature/humidity treatment. Before collecting thread strands, we placed 4 mm wide brass bars that were covered with double-sided carbon tape (product 77816, Electron Microscopy Sciences, Hatfield, PA, USA) between the ring's rim and center bar along web radii. This further isolated and stabilized the web sample and ensured that the tension of viscous threads adjacent to the ones being collected was not altered. Forceps, which were blocked open at a distance to accommodate the supports on which thread strands would be suspended, were used to collect individual capture spiral threads and transfer them to a microscope slide sampler. Double-sided carbon tape on the forceps' tips held each thread strand securely when the thread was burned free using a hot wire probe. Five U-shaped brass struts were epoxied at 4.8 mm intervals to microscope slides with their free ends extending upward and covered with double-sided carbon tape [fig. 3 in Opell et al. (Opell et al., 2011a)]. The forceps' tips were inserted into the Us of adjacent supports, allowing threads to be secured to the tops of their tape-covered supports.

To ensure that the probe used to extend droplets only contacted a single droplet at a time, we used a minuten insect pin moistened with distilled water to move away droplets that were adjacent to the test droplet located at the center of the thread strand. This process retained the aqueous coating of the strand's axial fibers, as demonstrated by the formation of small droplets similar to those often present between the large primary droplets of many viscous threads.

Humidity and temperature control

Thread samples were placed in a glass-covered aluminum observation chamber whose humidity was controlled as described previously [see fig. 4 in Opell et al. (Opell et al., 2011b)] and monitored with a Fisher Scientific Instant Digital Hygrometer. A Pletier thermo-electric unit mounted on the rear wall of this chamber and controlled by a thermostat permitted the temperature within the chamber to be controlled to ±1°C. Small auxiliary heating or cooling blocks were placed on the observation window to prevent the condensation of water vapor on the glass's inner surface.

We chose 20°C to represent early to mid-morning temperatures and 30°C to represent mid-day and afternoon temperatures (Fig. 2). At humidities above 90%, threads tended to pull free from the tape on the slide; therefore, morning humidity was simulated by 85% RH. Afternoon humidity was simulated by 50% RH, as a previous study suggests that optimal humidity for *A. aurantia* is below 60% (Opell et al., 2013). Hot & humid conditions were simulated by 30°C and 85% RH. Although realistic, these values are probably a conservative portrayal of morning and afternoon environmental differences.

Droplet extension and volume

Prior to extension, we photographed an isolated suspended droplet and determined its volume as described below. A steel probe was then inserted through a port in the side of the test chamber and its 413-µm-wide polished tip aligned and brought into contact with the focal droplet. To ensure full droplet adhesion, the probe was pressed against the droplet until the thread was deflected by a distance of 500 µm. A 60 frames s^{-1} video then recorded the probe's withdrawal at a velocity of 69.6 µm s^{-1} as a stepping motor moved the microscope stage, on which the chamber rested, pulling the droplet away from the stationary probe.

Dimensions from five droplets for each individual in each treatment replication were recorded, including the two droplets that were extended, and then averaged to determine how experimental conditions affected droplet volume. Only the values of extended droplets were used to determine whether droplet size correlated with droplet performance. We used ImageJ (Rasband, 1997-2012) to measure droplet length (L_d; dimension parallel to the axial fiber) and droplet width (W_d), from which we calculated droplet volume (V_d) using the following formula from a previous study (Opell and Schwend, 2007):

$$V_d = (2\pi\, W_d^2 L_d) / 15\,. \quad (1)$$

Droplet extension and axial line angle defection

The total loaded time (TLT) of droplet extension begins when the axial line is deflected from its initial non-loaded, 180 deg configuration and ends when the droplet returns to a non-loaded condition. TLT was divided into two phases; the pre-extension (PE) phase, during which a droplet exhibited tensive axial line deflection, but did not extend, thus holding the axial line in contact with the probe, and the droplet extension (DE) phase, which began when a droplet filament started to form and ended when the axial line returned to its 180 deg configuration at the end of TLT (Fig. 4).

During DE, we measured five axial line deflection angles: the angle at the start initiation of this phase, and the angles at 25, 50, 75 and 99% of the total duration time of DE, using iMovie ’11 (Apple Inc. 2010) and ImageJ. Subtracting the angle of axial line deflection from 180 deg produces an index that is directly proportional to the tension on the extending droplet filament.

Analysis

We analyzed the data for this study using JMP (SAS Institute, Cary, NC, USA) and considered comparisons with $P \leq 0.05$ as significant. Normally distributed values (as confirmed by Shapiro–Wilk W-tests with $P \geq 0.05$) were compared using ANOVA and t-tests. If the data were not normal, they were log-transformed, and once again tested for normality, and their transformed values were then compared using ANOVA. The Wilcoxon signed-rank test was used when values were not normally distributed.

Acknowledgements

Carlyle C. Brewster assisted with statistical analyses.

Competing interests

The authors declare no competing financial interests.

Author contributions

S.D.S. collected and prepared thread samples, performed droplet extensions and image measurements, analyzed data, and prepared the manuscript and figures. B.D.O. designed and constructed the instrumentation used in this study, and contributed to data analysis and manuscript and figure preparation. K.G.S. assisted with thread collection, droplet extension, image measurements and data entry.

Funding

Funds from the State Council for Higher Education for Virginia provided the digital camera used in this study.

References

Agnarsson, I. and Blackledge, T. A. (2009). Can a spider web be too sticky? Tensile mechanics constrains the evolution of capture spiral stickiness in orb-weaving spiders. *J. Zool. (Lond.)* **278**, 134-140.

Apstein, C. H. (1889). Bau und function der spinnendrusen der araneida. *Archiv Naturgeschichte* **1889**, 29-40.

Betz, O. and Kölsch, G. (2004). The role of adhesion in prey capture and predator defence in arthropods. *Arthropod Struct. Dev.* **33**, 3-30.

Blackledge, T. A. and Eliason, C. M. (2007). Functionally independent components of prey capture are architecturally constrained in spider orb webs. *Biol. Lett.* **3**, 456-458.

Blackledge, T. A. and Zevenbergen, J. M. (2006). Mesh width influences prey retention in spider orb webs. *Ethology* **112**, 1194-1201.

Boys, C. V. (1889). Quartz fibres. *Nature* **40**, 247-251.

Cambillau, C. (1995). The structural features of protein-carbohydrate interactions revealed by X-ray crystallography. In *Glycoproteins* (ed. J. V. Montreuil, J. F. G. Vliegenthart and H. Schachter), pp 59-61. New York, NY: Elsevier.

Choresh, O., Bayarmagnai, B. and Lewis, R. V. (2009). Spider web glue: two proteins expressed from opposite strands of the same DNA sequence. *Biomacromolecules* **10**, 2852-2856.

Edmonds, D. and Vollrath, F. (1992). The contribution of atmospheric water vapour to the formation and efficiency of a spider’s web. *Proc. R. Soc. B* **248**, 145-148.

Gosline, J. M., DeMont, M. E. and Denny, M. W. (1986). The structure and properties of spider silk. *Endeavour* **10**, 37-43.

Harmer, A. M. T., Blackledge, T. A., Madin, J. S. M. and Herberstein, M. E. (2011). High-performance spider webs: integrating biomechanics, ecology and behaviour. *J. R. Soc. Interface* **8**, 457-471.

Harwood, R. H. (1974). Predatory behavior of *Argiope aurantia* (Lucas). *Am. Midl. Nat.* **91**, 130-139.

Kappner, I., Al-Moghrabi, S. M. and Richter, C. (2000). Mucus-net feeding by the vermetid gastropod *Dendropoma maxima* in coral reefs. *Mar. Ecol. Prog. Ser.* **204**, 309-313.

Kelly, S. P., Sensenig, A., Lorentz, K. A. and Blackledge, T. A. (2011). Damping capacity is evolutionarily conserved in the radial silk of orb-weaving spiders. *Zoology* **114**, 233-238.

Opell, B. D. and Hendricks, M. L. (2007). Adhesive recruitment by the viscous capture threads of araneoid orb-weaving spiders. *J. Exp. Biol.* **210**, 553-560.

Opell, B. D. and Hendricks, M. L. (2009). The adhesive delivery system of viscous capture threads spun by orb-weaving spiders. *J. Exp. Biol.* **212**, 3026-3034.

Opell, B. D. and Schwend, H. S. (2007). The effect of insect surface features on the adhesion of viscous capture threads spun by orb-weaving spiders. *J. Exp. Biol.* **210**, 2352-2360.

Opell, B. D., Markley, B. J., Hannum, C. D. and Hendricks, M. L. (2008). The contribution of axial fiber extensibility to the adhesion of viscous capture threads spun by orb-weaving spiders. *J. Exp. Biol.* **211**, 2243-2251.

Opell, B. D., Tran, A. M. and Karinshak, S. E. (2011a). Adhesive compatibility of cribellar and viscous prey capture threads and its implication for the evolution of orb-weaving spiders. *J. Exp. Zool.* **315A**, 376-384.

Opell, B. D., Karinshak, S. E. and Sigler, M. A. (2011b). Humidity affects the extensibility of an orb-weaving spider’s viscous thread droplets. *J. Exp. Biol.* **214**, 2988-2993.

Opell, B. D., Karinshak, S. E. and Sigler, M. A. (2013). Environmental response and adaptation of glycoprotein glue within the droplets of viscous prey capture threads from araneoid spider orb-webs. *J. Exp. Biol.* **216**, 3023-3034.

Plateau, J. (1873). *Statique Expérimentale et Théorique des Liquides Soumis Aux Seules Forces Moléculaires*. Paris: Gauthier-Villars.

Rayleigh, J. W. S. (1892). Scientific papers. *Cambridge University Press* **3**, 585-596.

Reed, C. F., Witt, P. N. and Scarboro, M. B. (1969). The orb web during the life of *Argiope aurantia* (Lucas). *Dev. Psychobiol.* **2**, 120-129.

Rhodes, J. M. and Ching, C. K. (1993). The application of lectins to the study of mucosal glycoproteins. In *Glycoprotein Analysis in Biomedicine* (ed. E. F. Hounsell), pp. 247-262. New York, NY: Humana Press.

Sahni, V., Blackledge, T. A. and Dhinojwala, A. (2010). Viscoelastic solids explain spider web stickiness. *Nat. Commun.* **1**, 19.

Sahni, V., Blackledge, T. A. and Dhinojwala, A. (2011). Changes in the adhesive properties of spider aggregate glue during the evolution of cobwebs. *Sci. Rep.* **1**, 41.

Sekiguchi, K. (1952). On a new splnning gland found in geometric splders and its function. *Annot. Zool. Japonenses* **25**, 394-399.

Sensenig, A., Agnarsson, I. and Blackledge, T. A. (2010). Behavioural and biomaterial coevolution in spider orb webs. *J. Evol. Biol.* **23**, 1839-1856.

Sensenig, A. T., Lorentz, K. A., Kelly, S. P. and Blackledge, T. A. (2012). Spider orb webs rely on radial threads to absorb prey kinetic energy. *J. R. Soc. Interface* **9**, 1880-1891.

Sensenig, A. T., Kelly, S. P., Lorentz, K. A., Lesher, B. and Blackledge, T. A. (2013). Mechanical performance of spider orb webs is tuned for high-speed prey. *J. Exp. Biol.* **216**, 3388-3394.

Tillinghast, E. K., Townley, M. A., Wight, T. N., Uhlenbruck, G. and Janssen, E. (1992). The adhesive glycoprotein of the orb web of *Argiope aurantia* (Araneae, Araneidae). *MRS Proc.* **292**, 9-23.

Warburton, C. (1890). The spinning apparatus of geometric spiders. *Q. J. Microsc. Sci.* **31**, 29-39.